JBC RESEARCH ARTICLE

Ubiquitin-conjugating activity by PEX4 is required for efficient protein transport to peroxisomes in *Arabidopsis thaliana*

Received for publication, November 14, 2021, and in revised form, May 10, 2022 Published, Papers in Press, May 17, 2022,
https://doi.org/10.1016/j.jbc.2022.102038

Shoji Mano[1,2,*], **Yasuko Hayashi**[3], **Kazumi Hikino**[1], **Masayoshi Otomo**[3], **Masatake Kanai**[1], **and Mikio Nishimura**[1]

From the [1]*Department of Cell Biology, National Institute for Basic Biology, Myodaiji, Okazaki, Japan;* [2]*Department of Basic Biology, School of Life Science, SOKENDAI (The Graduate University for Advanced Studies), Myodaiji, Okazaki, Japan;* [3]*Graduate School of Science and Technology, Niigata University, Ikarashi, Niigata, Japan*

Edited by Joseph Jez

Protein transport to peroxisomes requires various proteins, such as receptors in the cytosol and components of the transport machinery on peroxisomal membranes. The Arabidopsis *apem* (*aberrant peroxisome morphology*) mutant *apem7* shows decreased efficiency of peroxisome targeting signal 1–dependent protein transport to peroxisomes. In *apem7* mutants, peroxisome targeting signal 2–dependent protein transport is also disturbed, and plant growth is repressed. The *APEM7* gene encodes a protein homologous to peroxin 4 (PEX4), which belongs to the ubiquitin-conjugating (UBC) protein family; however, the UBC activity of *Arabidopsis* PEX4 remains to be investigated. Here, we show using electron microscopy and immunoblot analysis using specific PEX4 antibodies and *in vitro* transcription/translation assay that PEX4 localizes to peroxisomal membranes and possesses UBC activity. We found that the substitution of proline with leucine by *apem7* mutation alters ubiquitination of PEX4. Furthermore, substitution of the active-site cysteine residue at position 90 in PEX4, which was predicted to be a ubiquitin-conjugation site, with alanine did not restore the *apem7* phenotype. Taken together, these findings indicate that abnormal ubiquitination in the *apem7* mutant alters ubiquitin signaling during the process of protein transport, suggesting that the UBC activity of PEX4 is indispensable for efficient protein transport to peroxisomes.

Peroxisomes are ubiquitous organelles that are present in most eukaryotic cells. In higher plants, peroxisomes differentiate into several classes according to cell type and developmental stage (1), and they are involved in various biological metabolic processes, such as fatty acid β-oxidation, photorespiration, and detoxification of reactive oxygen species (2, 3). Peroxisomes do not have their own genomes, and all peroxisomal proteins are encoded in the nuclear genome. Therefore, efficient and exact protein transport to peroxisomes is required to support various peroxisome functions. Peroxisomal matrix proteins are transported into the peroxisome after translation in the cytosol. There are two types of peroxisome targeting signals (PTSs): PTS1, located at the carboxyl terminus (4–8), and PTS2 in the extension sequence of precursor proteins located near the amino terminus (9–12). *PEROXIN* (*PEX*) genes are responsible for peroxisome biogenesis, including protein transport from yeast, mammalian cultured cells, and plants (13–19). PEX5 and PEX7 function as the PTS1 and PTS2 receptors, respectively, in yeast (20, 21), mammals (22, 23), and plants (24–30). These receptors recognize PTS1 or PTS2, bind to them in the cytosol, and direct them to the transport machinery consisting of PEX14 (31), PEX12 (16, 32), PEX13 (16, 32), and other unidentified factors on the peroxisomal membrane. After dissociation of matrix proteins and receptors, each receptor is recycled from peroxisomes to the cytosol and engages in the next round of protein transport; some PEXs, including PEX1, PEX2, PEX4, PEX6, PEX10, and PEX12, are involved in the transport of receptors from peroxisomes to the cytosol, as observed in yeast and mammalian cultured cells (33–37).

PEX4 genes were originally identified in *Saccharomyces cerevisiae* as *PAS2* (38), in *Pichia pastoris* as *PAS4* (39), and in *Hansenula polymorpha* as *PER2* (40) in a screening of mutants showing growth defects when cultured under a limited carbon source. The defect of PAS2 results in impaired growth of the yeast on medium containing oleic acid as the sole carbon source, mislocalization of peroxisomal matrix proteins, and the absence of functional peroxisomes (38). Similarly, *pas4* and *per2* mutants are unable to grow on medium containing methanol as the sole carbon source (39, 40). *PEX4* gene products belong to the ubiquitin-conjugating (UBC) protein family (38). UBC proteins function as E2 enzymes in the ubiquitin-conjugation cascade. UBC proteins accept ubiquitin from a ubiquitin-activating enzyme (E1) and transfer the ubiquitin molecule to the lysine residue of a target protein, which occurs either directly or through the action of a ubiquitin-protein ligase (E3) (41). Ubiquitin attaches to UBC proteins *via* a thioester bond between the carboxyl group at the carboxyl terminal glycine of ubiquitin and the active-site cysteine residue in the UBC protein. The cysteine residue is conserved among all UBC proteins and essential for the enzymatic activity (42). Analysis of yeast mutants shows that

* For correspondence: Shoji Mano, mano@nibb.ac.jp.
Present address for Mikio Nishimura: Department of Biology, Faculty of Science and Engineering, Konan University, Kobe 658-8501, Japan.

the UBC activity of PEX4 is necessary for the recycling of PEX5 from peroxisomes to the cytosol (43–45). Proteins homologous to PEX4 have not been identified in mammalian genomes such as human, mouse, and rat, whereas they have been identified in several plant species, such as *Arabidopsis thaliana*, *Oryza sativa*, *Populus trichocarpa*, and *Physcomitrella patens*. In *Arabidopsis*, Zolman *et al.* (34) identified the *PEX4* gene in an analysis of inodole-3-butyric acid–response mutants and showed that the defect of PEX4 causes inhibition of normal root hair growth. However, a biochemical characterization of plant PEX4, including its UBC activity, has not been performed to date.

In previous work, we investigated the molecular mechanisms of peroxisome biogenesis using *Arabidopsis apem* mutants and found that *apem1* and *apem3*, which are defective in dynamin-related protein 3A and peroxisomal membrane protein 38, respectively, cause elongation and enlargement of peroxisomes, indicating defects of peroxisome proliferation (15, 17). Analysis of *apem2*, *apem4*, and *apem9* mutants indicated that the *APEM2*, *APEM4*, and *APEM9* genes encode proteins homologous to PEX13, PEX12, and a Pex15p/PEX26 homolog, respectively, which function in protein transport to peroxisomes (16, 18). In addition, we presented evidence that the coordinated function of APEM10/Lon protease 2 in pexophagy is indispensable for quality control of peroxisomes (19, 46). Here, we report the isolation of another *apem* mutant, *apem7*, which is characterized by decreased efficiency of protein transport to peroxisomes. We show that the *APEM7* gene encodes PEX4, and that PEX4 has UBC activity. We also analyzed the relationship between PEX4-dependent ubiquitination and protein transport to peroxisomes *in planta*. The present findings indicate that the ubiquitination activity of APEM7/PEX4 on peroxisomal membranes is necessary for protein transport to peroxisomes.

Results

Decrease of efficiency of PTS1- and PTS2-dependent protein transport in the apem7 *mutant*

Arabidopsis apem mutants were screened from the pool of ethylmethanesulfonate-mutagenized transgenic *Arabidopsis* plants (termed GFP-PTS1), which expressed the peroxisome marker *GFP-PTS1*. We isolated a number of mutants that showed different GFP fluorescence pattern under the fluorescence microscope. The *apem* mutants were classified into four classes. These were mutants with (1) elongated peroxisomes, (2) enlarged peroxisomes, (3) GFP fluorescence in the cytosol as well as in peroxisomes, and (4) different distributions of peroxisomes. Of them, analysis of the *apem7* mutant detected GFP fluorescence in the cytosol and peroxisomes as punctate structures (Fig. 1), whereas in the parent plant, GFP-PTS1, GFP fluorescence was detected in peroxisomes but not in the cytosol (Fig. 1). Because GFP-PTS1 is transported into peroxisomes *via* a PTS1-dependent pathway, the GFP fluorescence in the cytosol suggests that the *apem7* mutation slightly affects the protein transport through this pathway.

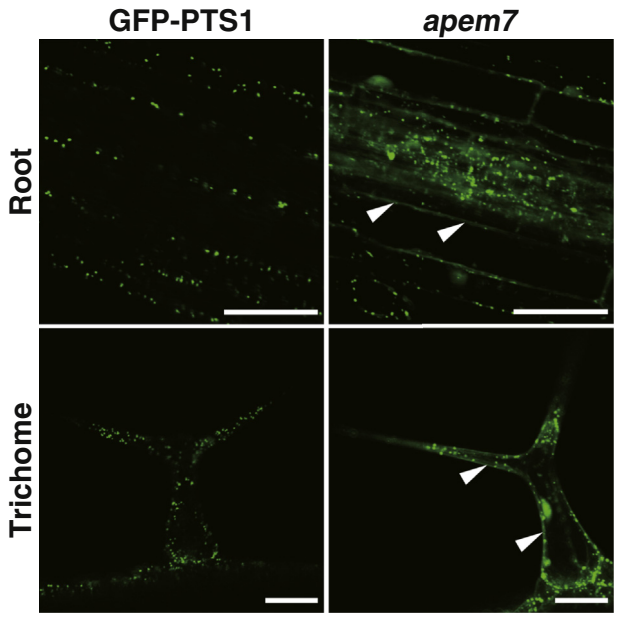

Figure 1. Cytosolic GFP fluorescence in *apem7* mutants. Peroxisomes were visualized as spherical structures in both GFP-PTS1 and *apem7* plants. In addition, GFP fluorescence was observed in the cytosol of *apem7* mutants. In root and trichome cells, central vacuole is so well developed that the fluorescence in cytosol between the cell wall and the vacuole is observed to frame the cell. Some representative cytosolic GFP is indicated by *arrowheads*. Bars represent 50 μm. *apem*, *aberrant peroxisome morphology*; PTS, peroxisome targeting signal 1.

In addition to the PTS1-dependent pathway, some peroxisomal matrix proteins are transported *via* a PTS2-dependent pathway (9–12). 3-Ketoacyl-CoA thiolase is a PTS2-containing protein that is translated as a high-molecular weight precursor protein in the cytosol and then transported into peroxisomes, where the amino-terminal PTS2-containing extension sequence is cleaved (47). For example, *apem2*, *apem4*, and *apem9* mutants are defective in PTS2-dependent protein transport, resulting in the accumulation of high-molecular weight precursor proteins, whereas these precursor proteins are hardly detected in WT plants (16, 18). In *apem7* mutants, small amounts of the precursor protein of 3-ketoacyl-CoA thiolase were detected (*arrowheads* in Fig. 2, *A* and *B*), indicating that PTS2-dependent protein transport is also slightly affected in *apem7* mutants. However, the level of protein accumulation was almost the same for PTS1-containing (isocytolate lyase, hydroxypyruvate reductase, and glycolate oxidase in Fig. 2*A*) and PTS2-containing (Thio in Fig. 2*A*) proteins. Overall, these results suggest that the *apem7* mutation affects protein transport to peroxisomes *via* both PTS1- and PTS2-dependent pathways, whereas it does not alter the total peroxisomal protein content of the cell.

Peroxisomal functions in apem7 *mutants*

We investigated whether the *apem7* mutation affects plant growth and peroxisomal functions, and the results showed that plant growth was repressed in *apem7* mutants compared with GFP-PTS1 plants (Fig. 3, *A* and *B*).

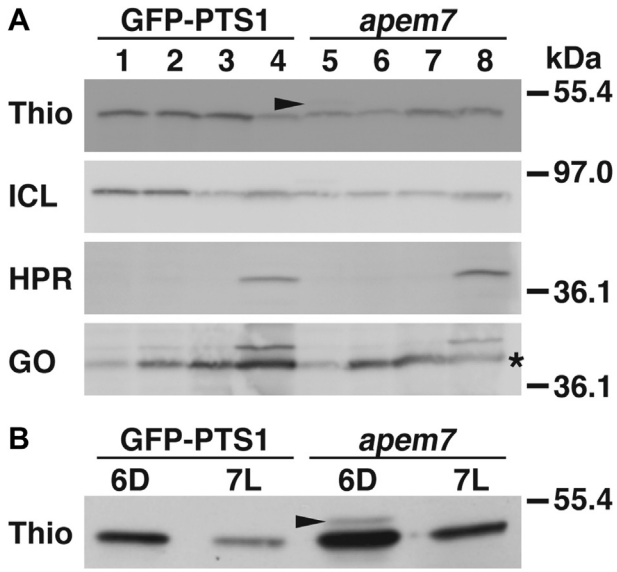

Figure 2. Immunodetection of peroxisomal proteins. *A*, GFP-PTS1 parent plant and *apem7* mutants were grown under continuous darkness for 3 days (lanes 1 and 5), 5 days (lanes 2 and 6), 7 days (lanes 3 and 7), or 2 days under continuous illumination after 5 days (lanes 4 and 8). Five micrograms of total protein were subjected to immunoblotting using antibodies against 3-ketoacyl CoA thiolase (Thio), isocytolate lyase (ICL), hydroxypyruvate reductase (HPR), and glycolate oxidase (GO). *B*, 10 μg of total protein prepared from 6-day-old plants under continuous darkness (6D) and 7-day-old plants under continuous light (7L) were used for immunoblotting. The *arrowheads* and *asterisk* represent the positions of the precursor proteins of thiolase and the nonspecific band, respectively. *apem*, *aberrant peroxisome morphology*; PTS1, peroxisome targeting signal 1.

Oilseed plants such as *Arabidopsis* store lipids as substrates for the production of sucrose by gluconeogenesis, which is used as energy for postgerminative growth. Fatty acids are produced by lipases in oil bodies and transported to peroxisomes, where they are metabolized to succinate by β-oxidation and the glyoxylate cycle. Therefore, β-oxidation is essential for producing sucrose, and peroxisomal β-oxidation-defective mutants, such as *peroxisome defective 1* (*ped1*) mutants, cannot germinate without exogenously supplied sucrose (Fig. 3*C* and (34, 48)). Although *apem7* mutants, unlike the *ped1* mutant, were able to germinate on medium without sucrose, the root length was shorter than that of the GFP-PTS1 parent plant (Fig. 3*C*). However, the root length of both *apem7* and GFP-PTS1 plants was almost the same on medium containing sucrose (Fig. S1). As another assay of peroxisomal β-oxidation, we analyzed growth on medium supplemented with 2,4-dichlorophenoxybutyric acid (2,4-DB), which is metabolized to the herbicide 2,4-dichlorophenoxyacetic acid by peroxisomal β-oxidation. The growth of WT plants, but not that of *ped1* mutants, is suppressed on medium containing 2,4-DB (Fig. 3*D* and (48)). The root length of *apem7* mutants was slightly longer than that of GFP-PTS1 plants on medium containing 2,4-DB (Fig. 3*D*). This result is good agreement with the previous data indexing the protoauxin indole-3-butyric acid into active indole-3-acetic acid conversion (34). These results indicate that peroxisomal β-oxidation was slightly, but not completely, decreased in *apem7* mutants.

The APEM7 *gene encodes PEX4, a member of the UBC family*

The *apem7* mutation segregates as a monogenic recessive gene. Map-based cloning revealed that the *APEM7* gene is located between the F6A4 and F15A18 bacterial artificial chromosome (BAC) clones on chromosome 5. We examined the nucleotide sequences in this region in the *Arabidopsis* genome sequence project and identified *At5g25760* as a possible candidate for the *APEM7* gene, which encodes a protein annotated as PEX4. We found a single nucleotide substitution on *At5g25760* in *apem7*, which caused an amino acid substitution of the 123rd proline to leucine (Fig. 4*A*).

To confirm that we had identified the correct gene, the *apem7* mutant was transformed with the WT *PEX4* gene. GFP fluorescence was observed only in peroxisomes in T1 plants of *apem7* transformed with the *PEX4* gene in contrast to the cytosolic location in *apem7* mutants (Fig. 4*B*). In addition, T1 plants of *apem7* transformed with *PEX4* showed normal postgerminative growth (Fig. 4*C*). The same result was obtained when *PEX4* complementary DNA (cDNA) was expressed in the *apem7* background under the control of a constitutive 35S promoter from cauliflower mosaic virus (Fig. 4*C*). These results demonstrate that the *PEX4* gene can complement *apem7*, thus confirming that *APEM7* is *PEX4*.

PEX4 is localized on peroxisomal membranes

To determine the subcellular and suborganellar localization of PEX4, we generated antibodies against the amino-terminal fragment of PEX4 (Met1-Glu50). These antibodies detected an 18 kDa band, which is consistent with the deduced molecular mass of PEX4, in extracts from GFP-PTS1 and *apem7* mutants (*arrow* in Fig. 5*A*). An additional band was present in the extract from *apem7* mutants (*arrowhead* in Fig. 5*A*). This band is described in Figure 6 in more detail. The total proteins were divided into soluble and membrane fractions, which were validated by detecting GFP and PEX14 proteins (soluble and membrane proteins, respectively) (Fig. 5*B*). PEX4 was detected exclusively in the membrane fraction.

To investigate the suborganellar localization of PEX4, we performed immunoelectron microscopic analysis. *Arabidopsis* leaves were treated with antibodies against PEX4 (15 nm gold particles represented by *arrows*) as well as with catalase, a peroxisome matrix protein (10 nm gold particles represented by *arrowheads*). As shown in Figure 5*C*, large gold particles were detected near the membrane of organelles labeled with catalase. This result together with the aforementioned immunoblot analyses indicates that PEX4 is localized on peroxisomal membranes. Although neither a transmembrane domain nor a membrane-bound domain has been found in PEX4, it has been shown to bind to a membrane protein, PEX22 (34). Our results are consistent with the previous results (34).

PEX4 is ubiquitinated, and the apem7 *mutation disturbs the ubiquitination of PEX4* in vivo

PEX4 is a member of the UBC protein family and functions as an E2 enzyme in the ubiquitination process in yeast (38). A

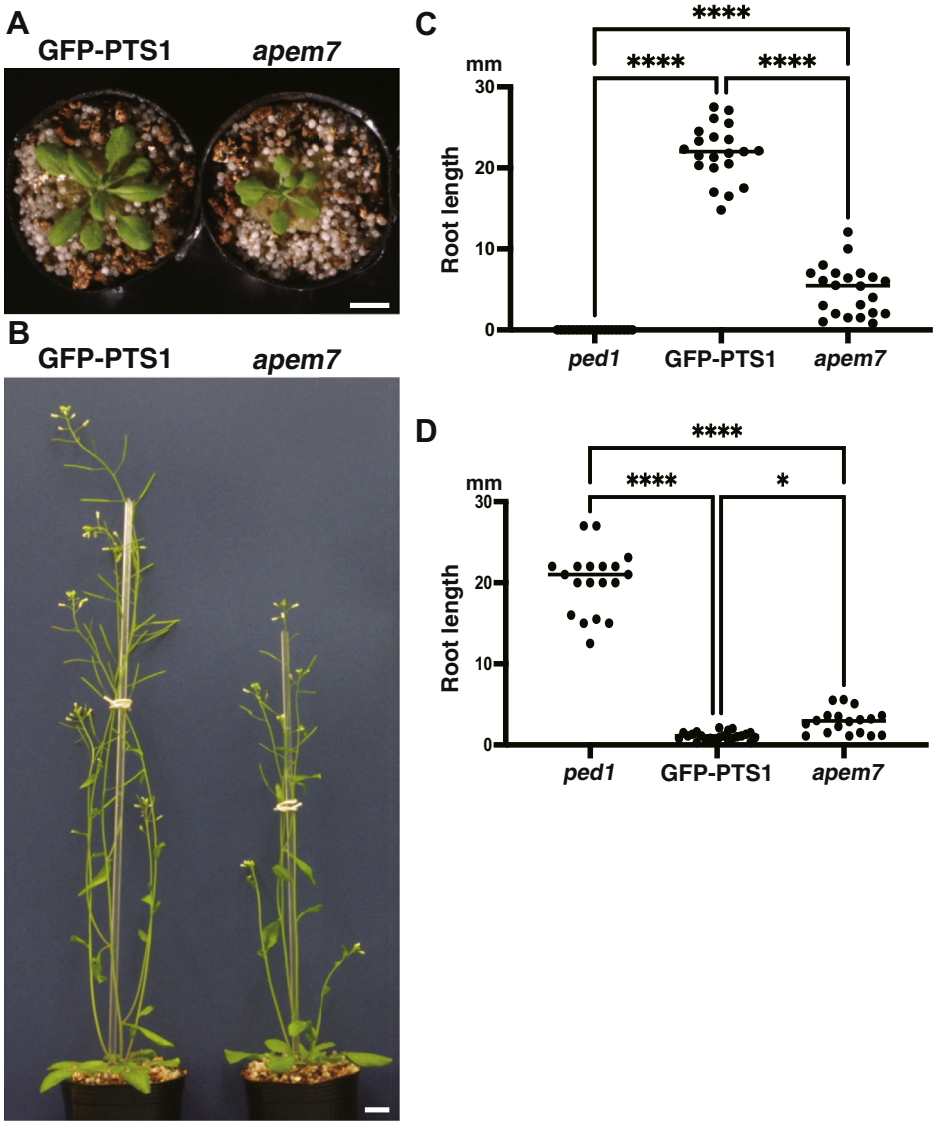

Figure 3. Phenotype of *apem7* mutants. *A*, 21-day-old and (*B*) 34-day-old plants grown under the light conditions are shown. Bars represent 1 cm. *C* and *D*, GFP-PTS1, *ped1*, and *apem7* mutants grown on medium without sucrose (*C*) or medium containing 2,4-DB (*D*) in the normal conditions. Statistical significance was analyzed by one-way ANOVA test. *$p < 0.05$, **$p < 0.01$, ***$p < 0.001$, and ****$p < 0.0001$. 2,4-DB, 2,4-dichlorophenoxybutyric acid; *apem*, *aberrant peroxisome morphology*; PTS1, peroxisome targeting signal 1.

search of public databases revealed that *Arabidopsis* PEX4 has sequence similarity to UBC proteins regarding the region surrounding the putative active-site cysteine residue that is essential for the formation of a thioester bond with ubiquitin (Fig. S2). If *Arabidopsis* PEX4 functions as an E2 enzyme, this protein should be ubiquitinated under nonreducing conditions because conjugation of ubiquitin to the E2 enzyme requires the formation of a thiol bond between ubiquitin and cysteine. To determine the state of PEX4 in the GFP-PTS1 plant and in the *apem7* mutant, we performed immunoblotting after SDS-PAGE under reducing or nonreducing conditions. The antibodies against PEX4 detected an 18 kDa polypeptide in the extracts from the parent plant, GFP-PTS1, and in *apem7* mutants under reducing conditions (lanes 1–3 in Fig. 6*A*). Because the *apem7* mutation causes an amino acid substitution, but it does not produce a termination codon, the polypeptides in the extracts from *apem7* mutants were thought to be mutated PEX4. In addition to an 18 kDa polypeptide, a 28 kDa polypeptide was detected under nonreducing conditions (lanes 4–6 in Fig. 6*A*). This 28 kDa polypeptide was not detected in GFP-PTS1 extracts under reducing conditions (lane 1 in Fig. 6*A*). The 28 kDa polypeptide was present in *apem7* mutants even under reducing conditions, although its amount was decreased (lane 2 in Fig. 6*A*). Expression of the *PEX4* gene dramatically reduced the amount of 28 kDa polypeptide in the *apem7* mutants (compare lane 3 with lane 6 in Fig. 6*A*), although a faint 28 kDa band was detected.

To investigate the 28 kDa polypeptide in more detail, we generated two mutated PEX4 constructs by substituting the 90th active-site cysteine residue with alanine or the 123rd *apem7*-mutation proline with leucine (PEX4C90A and PEX4P123L, respectively). We tried to synthesize WT

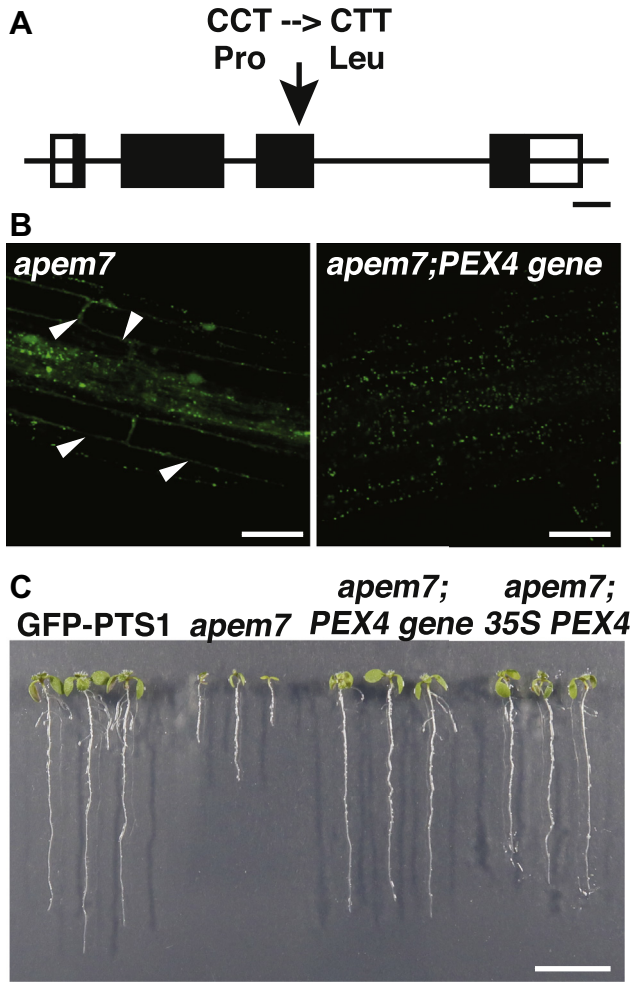

Figure 4. Positional cloning of the *APEM7* gene and rescue of the *apem7* phenotype. *A*, mutation position in the *apem7* mutant. The *apem7* mutation causes a nucleotide substitution of the 368th cytidine to thymidine (nucleotide residue 1 corresponds to the adenosine of the first methionine codon). Exons are indicated by *boxes*. Bar represents 100 bp. *B*, the *PEX4* gene restored the GFP fluorescence pattern in the *apem7* mutant. Some representative cytosolic GFP is indicated by *arrowheads*. Bars represent 50 μm. *C*, recovery of root growth of T1 plants of *apem7*;*PEX4* gene and *apem7*;35S:*PEX4*. Plants were grown for 7 days on medium without sucrose. Photographs were taken after the seedlings were removed from the medium and rearranged on agar plates. *apem*, *aberrant peroxisome morphology*; PEX4, peroxin 4.

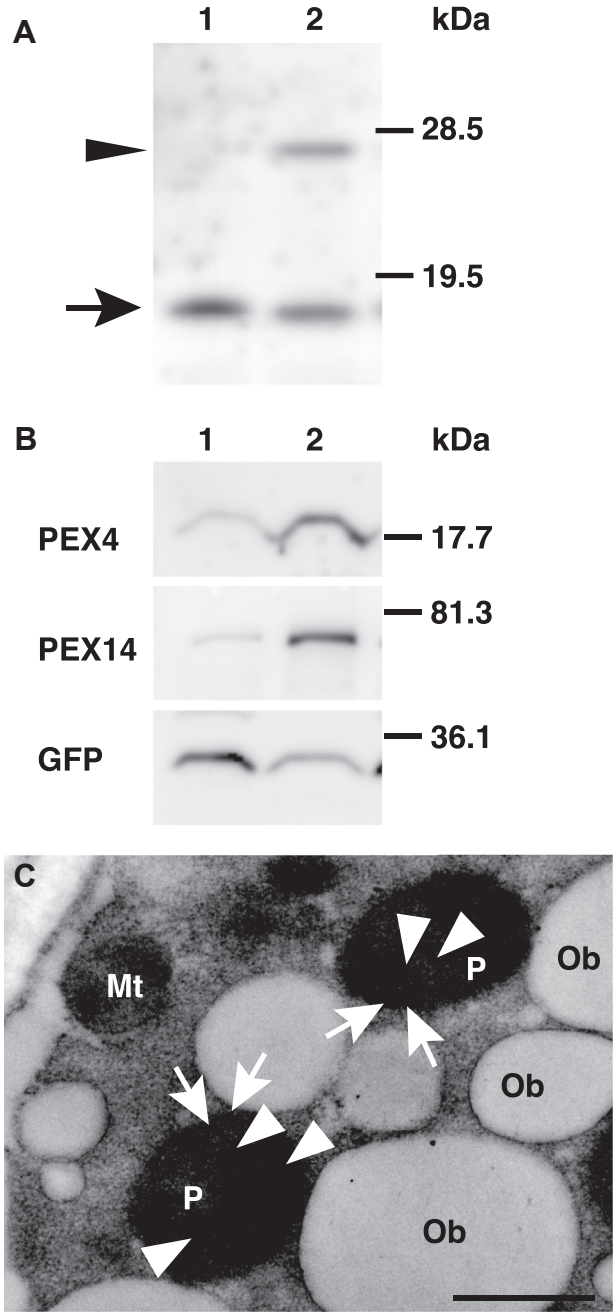

Figure 5. Immunodetection of PEX4 polypeptides and immunocytochemical localization of PEX4. *A*, 30 μg of total protein extracts from 7-day-old plants were used for immunoblot analysis with antibodies against PEX4. Lane 1: GFP-PTS1 plants; lane 2: *apem7* mutants. Molecular markers are indicated in kilodalton on the *right*. An *arrow* and an *arrowhead* on the *left* represent PEX4 and ubiquinated-PEX4, respectively. *B*, fractionation of total proteins into soluble and membrane fractions. Total proteins from the aerial parts of GFP-PTS1 plants grown for 13 days were fractionated into soluble and membrane fractions by centrifugation and immunoblotted for the indicated antibodies. Ten micrograms of protein were loaded on all lanes for PEX4 and PEX14, and 5 μg of protein was used for GFP. Lanes 1 and 2 represent soluble and membrane fractions, respectively. Molecular markers are indicated in kilodalton on the *right*. *C*, immunogold labeling of ultrathin sections of 3-day-old dark-grown cotyledons was performed using antibodies against PEX4 (15 nm, *arrows*) and catalase (10 nm, *open arrowheads*). Bar represents 500 nm. Mt, mitochondrion; Ob, oil body; P, peroxisome; PEX, peroxin; PTS1, peroxisome targeting signal 1.

(PEX4WT), PEX490A, and PEX4P123L proteins *in vitro* to investigate whether PEX4 could form conjugates with ubiquitin. Rabbit reticulocyte lysates are used for *in vitro* ubiquitination assays because they contain a rich source of ubiquitin, ubiquitin-activating E1 enzyme, and ATP (49). We therefore used rabbit reticulocyte lysates to express PEX4WT, PEX4C90A, and PEX4P123L and detected the polypeptides using PEX4 antibodies. In addition to the 18 kDa form of PEX4, a 28 kDa form of PEX4 was detected under nonreducing conditions (lane 6 in Fig. 6*B*). This 28 kDa form was not detected under reducing conditions in PEX4WT (lane 2 in Fig. 6*B*) and in PEXC90A even under nonreducing conditions (lane 7 in Fig. 6*B*). The 28 kDa form was still detected in PEX4P123L, which contains an amino acid substitution from proline to leucine in the *apem7* mutation (lane 8 in Fig. 6*B*). This 28 kDa peptide in PEX4P123L showed the same behavior as the 28 kDa form in PEX4WT (lane 4 in Fig. 6*B*). These

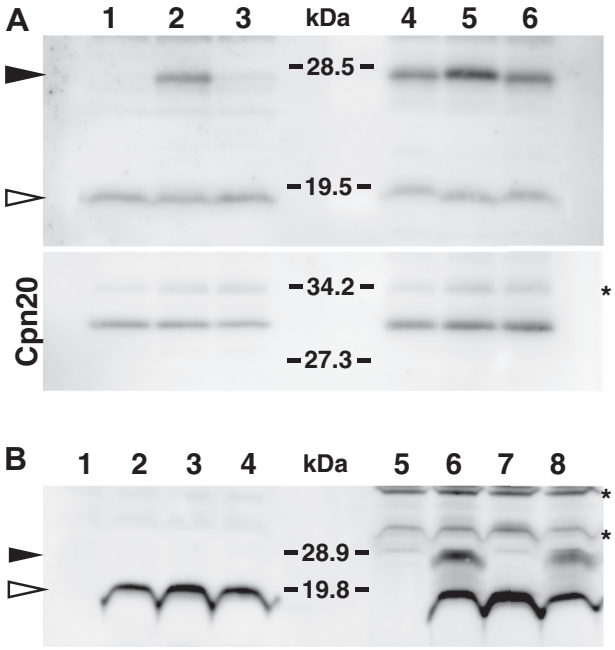

Figure 6. Enzymatic activity of PEX4 as a ubiquitin-conjugating enzyme. *A*, 30 μg of total extracts prepared from 7-day-old seedlings of GFP-PTS1 plants (lanes 1 and 4), *apem7* plants (lanes 2 and 5), and transgenic plants of *apem7*;*PEX4* gene (lanes 3 and 6) were used for immunodetection with antibodies against PEX4 under reducing (lanes 1–3) and nonreducing conditions (lanes 4–6). Chloroplast-Cpn20 antibody was used as a loading control for 10 μg of total extracts. *B*, WT (PEX4WT) and mutant *PEX4* cDNAs (PEX4C90A and PEX4P123L) were translated in a total volume of 12.5 μl using a rabbit reticulocyte lysate system, and each extract was divided into two fractions. After adding SDS sample buffer with and without β-mercaptoethanol, 7.5 μl was used for immunodetection with antibodies against PEX4. Lanes 1 and 5: empty vector as a negative control. Lanes 2 and 6: PEX4WT. Lanes 3 and 7: PEX4C90A. Lanes 4 and 8: PEX4P123L. Lanes 1 to 4: reducing conditions. Lanes 5 to 8: nonreducing conditions. *Open and closed arrowheads* represent PEX4 and ubiquitinated PEX4 polypeptides, respectively. *Asterisks* indicate nonspecific bands. Molecular markers are indicated in kilodalton on the center. *apem*, *aberrant peroxisome morphology*; cDNA, complementary DNA; PEX4, peroxin 4; PTS1, peroxisome targeting signal 1.

results indicate that PEX4 with the *apem7* mutation can accept a ubiquitin molecule as does WT PEX4. The same pattern of 18 and 28 kDa polypeptides was observed by autoradiography using [^{35}S]-labeled methionine, which was substituted with nonlabeled methionine in Figure 6*B* in rabbit reticulocyte lysates (Fig. S3). These results indicate that the 28 kDa form is a PEX4-ubiquitin conjugate and that the 90th cysteine functions as the ubiquitin-conjugation site.

To examine the role of UBC activity *in vivo*, *PEX4WT*, *PEX4C90A*, and *PEX4P123L* cDNAs were expressed in *apem7* mutants under the control of the *PEX4* promoter. As shown in Fig. S4, the fluorescence pattern in T1 plants expressing WT *PEX4* was the same as that of the parent plant GFP-PTS1 (Fig. S4, *A* and *B*), whereas fluorescence was observed in the cytosol and peroxisomes in T1 plants expressing *PEX4P123L* (Fig. S4, *C* and *D*) because the PEX4P123L is the *apem7* mutant-type protein. In T1 plants expressing *PEX4C90A*, the pattern of fluorescence was the same as that of PEX4P123L (Fig. S4, *E* and *F*). These results indicate that UBC activity is responsible for protein transport to peroxisomes *in vivo*.

Abnormal localization of PEX5 in apem*7 mutants*

PEX5 is essential for PTS1-dependent protein transport in *Arabidopsis* (28, 29). We previously reported that PEX5 accumulates at peroxisomal membranes in PTS1- and PTS2-dependent protein transport such as in *apem2* and *apem4* mutants (16). Therefore, we examined the localization of PEX5 in *apem7* mutants. In extracts from the parent plant GFP-PTS1, a large amount of PEX5 was detected in the soluble fraction, although small amounts of PEX5 were detected in the membrane fraction (lane 1 in Fig. 7). By contrast, the amount of membrane-associated PEX5 increased in *apem7* mutants (lane 4 in Fig. 7), and a minor portion was still detected in the soluble fraction. This result indicates that PEX5 binds to and does not move on peroxisomal membranes in *apem7* mutants.

PEX4 *is expressed in various tissues*

We examined the expression of *PEX4* using transgenic *Arabidopsis* plants harboring a *PEX4* promoter-*GUS* gene fusion. As shown in Figure 8, *GUS* expression was detected in various tissues at different developmental stages, which was mostly consistent with the data provided by public gene expression databases such as *Arabidopsis* eFP Browser (49) at the organ level. Figure 8 shows *GUS* expression at the tissue and cell levels. *PEX4* was strongly expressed in the veins of leaves and roots, especially in the vascular cylinder (Fig. 8, *A*–*D*, *F* and *H*), stigma (Fig. 8*E*), filaments of the stamen (Fig. 8*F*), septum (Fig. 8*G*), and root caps of main and lateral roots (Fig. 8, *B* and *H*). In addition, strong *PEX4* expression was observed in 3-day-old cotyledons, which have high peroxisomal β-oxidation activity (Fig. 8*H*), indicating a need for peroxisome functions in these organs and tissues.

Discussion

Here, we report the characterization of *Arabidopsis* PEX4 based on the analysis of the *apem7* mutant, which is defective in protein transport to peroxisomes. PEX4 belongs to the UBC protein family, although whether PEX4 has UBC activity was unclear. This study showed that PEX4 possesses UBC activity

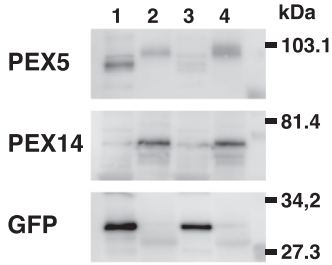

Figure 7. Membrane-associated PEX5 is increased in *apem7* mutant. Total proteins from 14-day-old GFP-PTS1 and *apem7* plants were fractionated into soluble and membrane fractions. Ten micrograms of protein were used for immunodetection. Lanes 1 and two represent soluble and membrane fractions from GFP-PTS1 plants, respectively. Lanes 3 and 4 represent soluble and membrane fractions from *apem7* mutants, respectively. Molecular markers are indicated in kilodalton on the *right*. *apem*, *aberrant peroxisome morphology*; PEX5, peroxin 5; PTS1, peroxisome targeting signal 1.

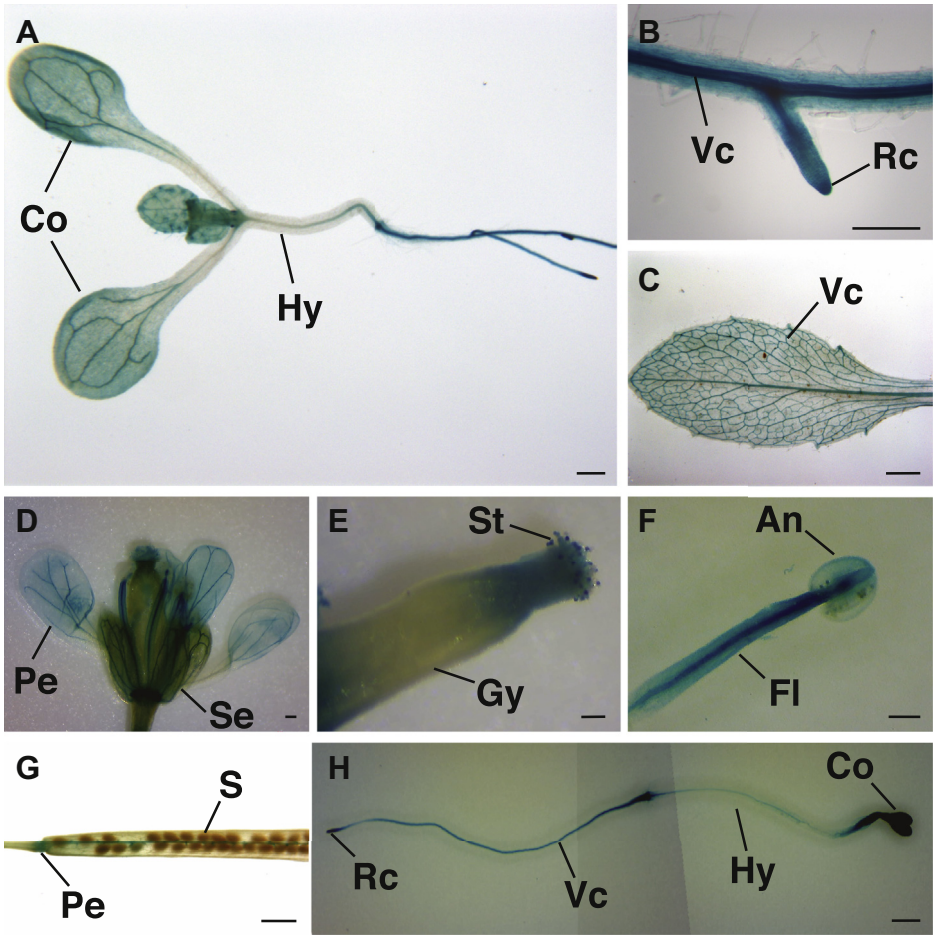

Figure 8. Histochemical analysis of *PEX4:GUS* reporter gene expression in various organs at different stages. Transgenic *Arabidopsis* plants harboring the *PEX4:GUS* construct were grown for 7 days in the light (*A* and *B*), 21 days in the light (*C*), 28 days in the light (*D–G*), and 3 days in the dark (*H*). *A* and *H*, seedlings. *B*, lateral root. *C*, cauline leaf. *D*, flower. *E*, pistil. *F*, stamen. *G*, fruit. Scale bars represent 1 mm (*A*, *C*, *D*, *F–H*) and 200 μm (*B* and *E*). *H*, two images were neatly connected and arranged. An, anther; Co, cotyledon; Fl, filament; Gy, gynoecium; Hy, hypocotyl; Pe, petal; PEX4, peroxin 4; Rc, root cap; S, seed; Se, sepal; St, stigma; Vc, vascular cylinder.

and defined the relationship between the state of ubiquitination of PEX4 and protein transport.

Effects of the apem7/pex4 *mutation on protein transport to peroxisomes*

The *Arabidopsis pex4* mutant was originally reported as *pex4-1* (34). The position of the *apem7* mutation is the same as that in *pex4-1*, suggesting that this position is the hot spot. The *apem7* mutation affects normal plant growth (Fig. 3) because it alters the transport of matrix proteins inside peroxisomes, which is essential for peroxisomal functions such as β-oxidation and photorespiration. Although some amounts of proteins are transported to peroxisomes, it may not be in enough amounts for various biological processes in peroxisomes. In the *H. polymorpha pex4* mutant, the typical PTS1 proteins, alcohol oxidase and dihydroxyacetone synthase, and catalase are predominantly present in the cytosol, whereas the PTS2 protein, amine oxidase, is located exclusively in peroxisomes (40). In *S. cerevisiae*, the *PEX4* null mutant shows impaired transport of thiolase and catalase (38). Taken together with these previous findings, the present results indicate that mutation and/or knockout of the *PEX4* gene affects the efficiency of protein transport.

In *apem7* mutants, the accumulation of peroxisomal proteins was not affected (Figs. 2 and 7). In *H. polymorpha pex4*, however, the major peroxisomal matrix proteins accumulate normally, whereas Pex3p, Pex5p, and Pex14p are increased, which may be due to a compensatory response to the import defect (40). Since *PEX4* is expressed in *Arabidopsis* at various stages of the tissue (Fig. 8), it remains possible that PEX4 is involved in protein accumulation in different peroxisomal proteins and tissues not investigated here.

Detection of UBC activity and the effect of PEX4 ubiquitination on protein transport

A cysteine residue conserved among plant and yeast PEX4s is assumed to be the ubiquitin-conjugation site (Fig. S2). In plants, however, there is no evidence supporting that PEX4 has UBC activity or that the conserved residue is essential for UBC activity. We detected an additional PEX4 polypeptide (Figs. 5 and 6) with a molecular size that was almost the same as that of ubiquitinated PEX4. This additional polypeptide was

sensitive to reducing agents such as β-mercaptoethanol (Fig. 6). When the conserved cysteine was replaced with alanine, this additional PEX4 polypeptide was not detected (Fig. 6). These results suggest that conjugation of ubiquitin to PEX4 occurs *via* the formation of a thioester bond at the 90th cysteine. This Cys90-dependent ubiquitination was detected even in the *apem7* mutant under nonreducing conditions (lane 2 in Fig. 6*A*). However, ubiquitinated PEX4 in the *apem7* mutant was detected even under reducing conditions (lane 6 in Fig. 6*A*), suggesting that PEX4 ubiquitination in the *apem7* mutant occurs at a different amino acid residue that is not affected by reducing agents or that the ubiquitin at the 90th Cys was not dissociated. The ubiquitination of *apem7* PEX4 (lane 4 in Fig. 6*B*) showed the same sensitivity to the reducing agent as that of WT PEX4 (lane 2 in Fig. 6*B*) *in vitro*. The difference between the *in vivo* (Fig. 6*A*) and *in vitro* (Fig. 6*B*) processes could be attributed to conditions related to PEX4, such as the accessibility of other factors interacting with PEX4 directly and indirectly. In addition to PEX4, several factors involved in the ubiquitination process in peroxisomes have been identified in *Arabidopsis*, such as PEX1 and PEX6 as AAA ATPases (36, 50–52); PEX2, PEX10, and PEX12 as ubiquitin ligases (16, 53–56); and PEX22 and APEM9 for tethering of PEX4 or the PEX1–PEX6 complex to peroxisomal membranes (18, 34). These factors are present on the peroxisomal membrane, and their defects result in decreased protein transport (16, 18, 36, 52). Therefore, the interaction of these factors with PEX4 may affect the ubiquitination status of PEX4 *in vivo*. The *apem7* mutation may alter the interactions with these and other unidentified factors, and/or the conformation of PEX4 itself, resulting in its ubiquitination even under reducing conditions.

In yeast and mammalian cells, the PTS1 receptor PEX5 is recycled from peroxisomes to the cytosol after dissociation of cargo proteins and then participates in the next round of protein transport (57, 58). There is currently no evidence supporting the existence of this recycling system in plant cells. However, in this study, the amount of membrane-associated PEX5 was increased in *Arabidopsis pex4* mutants (Fig. 7 (59)), which is consistent with the reports in yeast and mammalian cells (40, 43). Previous findings together with the present data indicate that ubiquitinated PEX4 at peroxisomal membranes and abnormal accumulation of PEX5 at peroxisomal membranes disturbs the recycling of the two receptors. As a result, receptor-dependent protein transport may fail to function normally. In yeast and mammalian cells, PEX5 is a target for ubiquitination (43–45, 60, 61). However, the final target proteins that are ubiquitinated *via* the PEX4-dependent system remain undefined in plants. We found that membrane-associated PEX5 had a slightly larger molecular size than PEX5 in the soluble fraction (compare lanes 1 and 2 in Fig. 7) and that the amount of this larger polypeptide was increased in the *apem7* mutant (lane 4 in Fig. 7). This suggests that *Arabidopsis* PEX5 is modified at the peroxisomal membrane, and it is possible that this modification is ubiquitination. *In vitro* UBC assay is a powerful tool to characterize E2 and E3 enzymes in the ubiquitin cascade, and this system has been widely used in plants (62–65). We attempted to perform this assay to characterize PEX4 but were unable to express the PEX4 protein in a soluble form in *Escherichia coli* or *via* an *in vitro* transcription/translation method, despite using different conditions. Kraft *et al.* (66) characterized *Arabidopsis* E2 and E3 enzymes by expressing proteins in *E. coli* or in insect cells. Among the proteins analyzed, the PEX4 UBC activity was not detected because the protein was obtained in the insoluble and not the soluble form (66). The present results are in good agreement with their report. A different system needs to be developed to obtain PEX4 proteins in an active soluble form to investigate PEX4-dependent ubiquitin signaling, which would considerably advance our understanding of the ubiquitination process at peroxisomes.

Experimental procedures

Plant materials

The GFP-PTS1 parent plants (accession Columbia), *apem7* mutants, and transgenic plants were grown as described previously (15).

Confocal microscopic observation

Tissues of GFP-PTS1 and *apem7* mutants were prepared and examined using an LSM510META laser-scanning confocal microscope (Carl Zeiss) as previously described (67).

Map-based cloning of the APEM7 locus

The *apem7* homozygotes were backcrossed three times with the parent plant GFP-PTS1 and then crossed with another accession, Landsberg *erecta*. A total of 29 F2 progenies expressing mutant phenotypes were scored according to their genetic background as revealed by a series of cleaved amplified polymorphic sequences and simple sequence length polymorphism markers, which were made according to the Monsanto Arabidopsis Polymorphism and Ler Sequence Collections (http://www.arabidopsis.org/browse/Cereon/index.jsp). Markers on BAC clones F6A4 and F15A18 indicated that the *APEM7* locus is located in the region between 17 BAC clones. Examination of the nucleotide sequences in this region identified *At5g25760* as a candidate locus. Based on this nucleotide sequence, the DNA fragments corresponding to this region were amplified from the genomic DNAs of a GFP-PTS1 plant and an *apem7* mutant using the same primer set and were fully sequenced.

Generation of transgenic plants

The *APEM7* gene conjugated at the KpnI and XhoI sites at the 5′ and 3′ ends, respectively, was amplified by PCR. The DNA fragment contained a 2340 bp upstream region, an open reading frame, and a 590 bp downstream region. The PCR-amplified fragments were then subcloned and sequenced. After digestion with KpnI and XhoI, the DNA fragments were inserted into the KpnI–XhoI site on the pENTR2B vector (Thermo Fisher Scientific), and the insert was then transferred to the binary vector pGWB1 (68) by an LR recombination

reaction (Thermo Fisher Scientific), generating pGW1APM7G.

To generate pGW2PEX4 bearing *PEX4* cDNA under the control of the constitutive 35S promoter from cauliflower mosaic virus, SalI–NotI sites were introduced into the 5′ and 3′ ends of *PEX4* cDNA, respectively, by PCR. Then, the SalI–NotI fragments were inserted into the SalI–NotI site on the pENTR2B vector (Thermo Fisher Scientific), and the insert was transferred to the binary vector pGWB2 (68) by an LR recombination reaction (Invitrogen).

To generate pPEX4pWT, pPEX4pC90A, and pPEX4pP123L, in which WT PEX4, PEX4 with 90th cysteine to alanine substitution, or PEX4 with 123rd proline to leucine substitution, respectively, was regulated under the *PEX4* promoter, site-directed mutagenesis was performed using WT *PEX4* cDNA. Each fragment was amplified by PCR to conjugate *att*B1 and *att*B2 sites at the 5′ and 3′ ends, respectively, and then transferred to the donor vector, pDONR221, by a BP recombination reaction (Thermo Fisher Scientific), generating the entry clones of p221PEX4WT, p221PEX4C90A, and p221PEX4P123L. DNA fragments containing the upstream region of *PEX4* (−1939 to +3) conjugated at *att*B4 and *att*B1R sites at the 5′ and 3′ ends, respectively, were amplified by PCR. The PCR-amplified fragments were transferred to the donor vector, pDONR P4-P1R, by a BP recombination reaction (Thermo Fisher Scientific), generating pPEX4pro-P4P1R. Each entry clone, pPEX4pro-P4P1R and R4pGWB501 (69), was subjected to LR recombination reaction.

Each vector was then transformed into *Agrobacterium tumefaciens* (strain C58C1Rif^R) by electroporation. The *apem7* mutants were transformed using the infiltration method (70). Transformants were selected on medium containing 50 μg/ml hygromycin.

To generate pAPM7GUS containing the fusion of the *PEX4* promoter with the β-glucuronidase gene, pPEX4pro-P4P1R and R4L1pGWB550 (71) were subjected to LR recombination reaction to generate pPEX4proGUS. pPEX4proGUS was used for transformation into WT *Arabidopsis* plants as described previously.

Preparation of antibodies against PEX4

A DNA fragment encoding the amino acid sequence from the first methionine to the 50th amino acid residue of PEX4 conjugated to BamHI and HindIII sites at the 5′ and 3′ ends, respectively, was amplified by PCR using *PEX4* cDNA as a template. The amplified DNA was digested with BamHI and HindIII and inserted into the pET32a vector (Novagen). A PEX4 and His-tag fusion protein was synthesized in *E. coli* cells (strain BL21), purified, and used for production of rabbit antibodies against PEX4 as described previously (72).

Immunoblot analysis

For extraction of total proteins, *Arabidopsis* cotyledons grown to various stages were homogenized with extraction buffer (20 mM Tris–HCl, pH 6.8, 2% SDS, and 24% glycerol), and the homogenates were centrifuged at 20,400*g* for 15 min at 4 °C.

Membranes were fractionated as described previously (73) with slight modifications. Briefly, the *Arabidopsis* cotyledons grown for 14 days were homogenized with buffer A (10 mM Hepes–KOH, pH 8.0, 10 mM $MgCl_2$, and a Protease Inhibitor Cocktail) (Boehringer Mannheim) and then centrifuged at 10,000*g* for 5 min at 4 °C to separate into soluble and membrane fractions. The membrane fractions were lysed in buffer B (10 mM Hepes–KOH, pH 8.0, 10 mM $MgCl_2$, 1 mM EDTA, 1% digitonin, and a Protease Inhibitor Cocktail) (Boehringer Mannheim) and centrifuged at 10,000*g* for 5 min at 4 °C again. The protein content of each extract was estimated using a protein assay kit (Bradford ULTRA; FUNAKOSHI) with bovine serum albumin as the standard protein. Each extract was divided into two fractions, and the same volume of SDS sample buffer with or without β-mercaptoethanol was added.

Proteins were separated by SDS-PAGE on a 7.5% or 15% polyacrylamide gel and transferred to a polyvinylidene difluoride membrane (Merck) in a semidry electroblotting system. Immunologic reactions were detected by monitoring the activity of horseradish peroxidase–coupled antibodies against rabbit immunoglobulin G (Chemi-Lumi One Super; Nacalai). Antibodies against chloroplast-Cpn20 (74) were used as a loading control in Figure 6*A*.

Electron microscopic analysis

The methods used for sample preparation and detection by electron microscopic analysis were described previously (75). Cotyledons from 3-day-old seedlings grown under dark conditions were frozen in a high-pressure freezing machine (HPM-010; Bal-Tec). After freeze substitution, cotyledons were embedded in LR white. Ultrathin sections (80 nm) of cells were obtained using a diamond knife ultramicrotome (EM UC7; Leica) and placed on nickel grids treated with 2% Bioden Mesh Cement (Okenshoji Co, Ltd). The one-side sections were immunoreacted with primary antibodies against *Arabidopsis* PEX4 (1:100 dilution [v/v]) for 8 h at 4 °C and then treated with protein A-gold (15 nm; BBInternational) as a secondary antibody for 60 min at room temperature, followed by washing with distilled water and drying. Subsequently, the other-side sections were immunoreacted with primary antibodies against catalase (1:1000 dilution [v/v]) for 3 h at room temperature, treated with protein A-gold (10 nm; BBInternational) as the secondary antibody for 60 min at room temperature, and then washed with distilled water and dried. Sections were stained with 4% uranyl acetate for 10 min at room temperature and examined under a transmission electron microscope (H-7650; Hitachi High-Tech Co) at 80 kV.

In vitro *transcription/translation for ubiquitination*

In vitro transcription/translation for ubiquitination was performed using a rabbit reticulocyte lysate system according to the method described (39) with slight modifications. WT *PEX4* and *PEX4* containing C90A or P123L mutation cDNAs were subcloned into the pBluescript SK(+) vector to generate

pSKPEX4WT, pSKPEX4C90A, and pSKPEX4P123L. Each plasmid was used for *in vitro* transcription/translation using TNT rabbit reticulocyte lysate (Promega) in the presence of [^{35}S]methionine according to the manufacturer's instructions. Each extract was divided into two fractions, mixed with SDS sample buffers with and without β-mercaptoethanol, boiled for 5 min, and separated by SDS-PAGE. The gels were washed with Tris–glycine buffer (25 mM Tris, 192 mM glycine, pH 8.3) briefly, dried onto a paper filter (Cytiva), and detected using BAS-5000 (Fujifilm). The same experiments were performed with nonradiolabeled methionine for immunoblot analysis using antibodies against PEX4.

Data availability

All data are available in the main text or in the supporting information.

Supporting information—This article contains supporting information.

Acknowledgments—We thank Drs Tsuyoshi Nakagawa (Shimane University) and Roger Y. Tsien (University of California, San Diego) for provision of experimental materials, Drs Junji Yamaguchi (Hokkaido University) and Takeo Sato (Hokkaido University) for technical advice on ubiquitination assays, and the staff of the center for radioisotope facilities and model plant facilities at the National Institute for Basic Biology for technical support. We are also grateful to Ms Chihiro Nakamori, Masami Araki, and Azusa Matsuda for supporting experiments and taking care of plants as technical staff.

Author contributions—S. M. and M. N. conceptualization; S. M., Y. H., K. H., and M. O. investigation; S. M., Y. H., and M. K. writing–original draft; M. N. writing–review & editing; S. M. supervision; S. M., project administration; S. M. funding acquisition.

Funding and additional information—This work was supported in part by the Japan Society for the Promotion of Science KAKENHI grant (grant numbers: 20059035, 22112523, 17K07457, and 20K06711; to S. M.; and 17K07467; to Y. H.).

Conflict of interest—The authors declare that they have no conflicts of interest with the contents of this article.

Abbreviations—The abbreviations used are: *apem*, *aberrant peroxisome morphology*; BAC, bacterial artificial chromosome; cDNA, complementary DNA; 2,4-DB, 2,4-dichlorophenoxybutyric acid; PEX4, peroxin 4; PTS, peroxisome targeting signal; UBC, ubiquitin-conjugating.

References

1. Kamada, T., Nito, K., Hayashi, H., Mano, S., Hayashi, M., and Nishimura, M. (2003) Functional differentiation of peroxisomes revealed by expression profiles of peroxisomal genes in *Arabidopsis thaliana*. *Plant Cell Physiol.* **44**, 1275–1289
2. Mano, S., and Nishimura, M. (2005) Plant peroxisomes. *Vit. Hor.* **72**, 111–154
3. Hu, J., Baker, A., Bartel, B., Linka, N., Mullen, R. T., Reumann, S., *et al.* (2012) Plant peroxisomes: biogenesis and function. *Plant Cell* **24**, 2279–2303
4. Gould, S. J., Keller, G.-A., and Subramani, S. (1987) Identification of a peroxisomal targeting signal at the carboxy terminus of firefly luciferase. *J. Cell Biol.* **105**, 2323–2931
5. Gould, S. J., Keller, G.-A., and Subramani, S. (1988) Identification of peroxisomal targeting signals located at the carboxy terminus of four peroxisomal proteins. *J. Cell Biol.* **107**, 897–905
6. Gould, S. J., Keller, G.-A., Hosken, N., Wilkinson, J., and Subramani, S. (1989) A conserved tripeptide sorts proteins to peroxisomes. *J. Cell Biol.* **108**, 1657–1664
7. Gould, S. J., Keller, G.-A., Schneider, M., Howell, S. H., Garrard, L. J., Goodman, J. M., *et al.* (1990) Peroxisomal protein import is conserved between yeast, plants, insects and mammals. *EMBO J.* **9**, 85–90
8. Hayashi, M., Aoki, M., Kondo, M., and Nishimura, M. (1997) Changes in targeting efficiencies of proteins to plant microbodies caused by amino acid substitutions in the carboxy-terminal tripeptide. *Plant Cell Physiol.* **38**, 759–768
9. Kato, A., Hayashi, M., Mori, H., and Nishimura, M. (1995) Molecular characterization of a glyoxysomal citrate synthase that is synthesized as a precursor of higher molecular mass in pumpkin. *Plant Mol. Biol.* **27**, 377–390
10. Kato, A., Hayashi, M., Kondo, M., and Nishimura, M. (1996) Targeting and processing of a chimeric protein with the N-terminal presequence of the precursor to glyoxysomal citrate synthase. *Plant Cell* **8**, 1601–1611
11. Kato, A., Takeda-Yoshikawa, Y., Hayashi, M., Kondo, M., Hara-Nishimura, I., and Nishimura, M. (1998) Glyoxysomal malate dehydrogenase in pumpkin: cloning of a cDNA and functional analysis of its presequence. *Plant Cell Physiol.* **39**, 186–195
12. Hayashi, H., Bellis, L. D., Yamaguchi, K., Kato, A., Hayashi, M., and Nishimura, M. (1998) Molecular characterization of a glyoxysomal long chain acyl-CoA oxidase that is synthesized as a precursor of higher molecular mass in pumpkin. *J. Biol. Chem.* **273**, 8301–8307
13. Fujiki, Y. (2000) Peroxisome biogenesis and peroxisome biogenesis disorders. *FEBS Lett.* **476**, 42–46
14. Holroyd, C., and Erdmann, R. (2001) Protein translocation machineries of peroxisomes. *FEBS Lett.* **501**, 6–10
15. Mano, S., Nakamori, C., Kondo, M., Hayashi, M., and Nishimua, M. (2004) An *Arabidopsis* dynamin-related protein, DRP3A, controls both peroxisomal and mitochondrial division. *Plant J.* **38**, 487–498
16. Mano, S., Nakamori, C., Nito, K., Kondo, M., and Nishimura, M. (2006) The Arabidopsis *pex12* and *pex13* mutants are defective in both PTS1- and PTS2-dependent protein transport to peroxisomes. *Plant J.* **47**, 604–618
17. Mano, S., Nakamori, C., Fukao, Y., Araki, M., Matsuda, A., Kondo, M., *et al.* (2011) A defect of peroxisomal membrane protein 38 causes enlargement of peroxisomes. *Plant Cell Physiol.* **52**, 2157–2172
18. Goto, S., Mano, S., Nakamori, C., and Nishimura, M. (2011) *Arabidopsis* ABERRANT PEROXISOME MORPHOLOGY9 is a peroxin that recruits the PEX1-PEX6 complex to peroxisomes. *Plant Cell* **23**, 1573–1587
19. Goto-Yamada, S., Mano, S., Yamada, K., Oikawa, K., Hosokawa, Y., Hara-Nishimura, I., *et al.* (2015) Dynamics of the light-dependent transition of plant peroxisomes. *Plant Cell Physiol.* **56**, 1264–1271
20. Leij, I. V. D., Franse, M. M., Elgersma, Y., Distel, B., and Tabak, H. F. (1993) PAS10 is a tetratricopeptide-repeat protein that is essential for the import of most matrix proteins into peroxisomes of *Saccharomyces cerevisiae*. *Proc. Natl. Acad. Sci. U. S. A.* **90**, 11782–11786
21. Marzioch, M., Erdmann, R., Veenhuis, M., and Kunau, W.-H. (1994) PAS7 encodes a novel yeast member of the WD-40 protein family essential for import of 3-oxoacyl-CoA thiolase, a PTS2-containing protein, into peroxisomes. *EMBO J.* **13**, 4908–4918
22. Fransen, M., Brees, C., Baumgart, E., Vanhooren, J. C. T., Baes, M., Mannaerts, G. P., *et al.* (1995) Identification and characterization of the putative human peroxisomal C-terminal targeting signal import receptor. *J. Biol. Chem.* **270**, 7731–7736
23. Wiemer, E. A. C., Lüers, G. H., Faber, K. N., Wenzel, T., Veenhuis, M., and Subramani, S. (1996) Isolation and characterization of Pas2p, a peroxisomal membrane protein essential for peroxisome biogenesis in the methylotrophic yeast *Pichia pastoris*. *J. Biol. Chem.* **271**, 18973–18980

24. Kragler, F., Lametschwandtner, G., Christmann, J., Hartig, A., and Harada, J. J. (1998) Identification and analysis of the plant peroxisomal targeting signal 1 receptor NtPEX5. *Proc. Natl. Acad. Sci. U. S. A.* **95**, 13336–13341
25. Wimmer, C., Schmid, M., Veenhuis, M., and Gietl, C. (1998) The plant PTS1 receptor: similarities and differences to its human and yeast counterparts. *Plant J.* **16**, 453–464
26. Schumann, U., Gietl, C., and Schmid, M. (1999) Sequence analysis of a cDNA encoding Pex7p, a peroxisomal targeting signal 2 receptor from Arabidopsis. *Plant Physiol.* **120**, 339
27. Gurvitz, A., Wabnegger, L., Langer, S., Hamilton, B., Ruis, H., and Hartig, A. (2001) The tetraricopeptide repeat domains of human, tobacco, and nematode PEX5 proteins are functionally interchangeable with the analogous native domain for peroxisomal import of PTS1-terminated proteins in yeast. *Mol. Gen. Genet.* **265**, 276–286
28. Hayashi, M., Yagi, M., Nito, K., Kamada, T., and Nishimura, M. (2005) Differential contribution of two peroxisomal protein receptors to the maintenance of peroxisomal functions in *Arabidopsis*. *J. Biol. Chem.* **280**, 14829–14835
29. Nito, K., Hayashi, M., and Nishimura, M. (2002) Direct interaction and determination of binding domains among peroxisomal import factors in *Arabidopsis thaliana*. *Plant Cell Physiol.* **43**, 355–366
30. Woodward, A. W., and Bartel, B. (2005) The *Arabidopsis* peroxisomal targeting signal type 2 receptor PEX7 is necessary for peroxisome function and dependent on PEX5. *Mol. Biol. Cell* **16**, 573–583
31. Hayashi, M., Nito, K., Toriyama-Kato, K., Kondo, M., Yamaya, T., and Nishimura, M. (2000) *At*Pex14p maintains peroxisomal functions by determining protein targeting to three kinds of plant peroxisomes. *EMBO J.* **19**, 5701–5710
32. Fan, J., Quan, S., Orth, T., Awai, C., Chory, J., and Hu, J. (2005) The Arabidopsis *PEX12* gene is required for peroxisome biogenesis and is essential for development. *Plant Physiol.* **139**, 231–239
33. Zolman, B. K., and Bartel, B. (2004) An *Arabidopsis* indole-3-butyric acid-response mutant defective in PEROXIN6, an apparent ATPase implicated in peroxisomal function. *Proc. Natl. Acad. Sci. U. S. A.* **101**, 1786–1791
34. Zolman, B. K., Monroe-Augustus, M., Silva, I. D., and Bartel, B. (2005) Identification and functional characterization of Arabidopsis PEROXIN4 and the interacting protein PEROXIN22. *Plant Cell* **17**, 3422–3435
35. Hasan, S., Platta, H. W., and Erdmann, R. (2013) Import of proteins into the peroxisomal matrix. *Front. Physiol.* **4**, 261
36. Rinaldi, M. A., Fleming, W. A., Gonzalez, K. L., Park, J., Ventura, M. J., Patel, A. B., *et al.* (2017) The PEX1 ATPase stabilizes PEX6 and plays essential roles in peroxisome bology. *Plant Physiol.* **174**, 2231–2247
37. Baker, A., Lanyon-Hogg, T., and Warriner, S. L. (2016) Peroxisome protein import: a complex journey. *Biochem. Soc. Trans.* **44**, 783–789
38. Wiebel, F. F., and Kunau, W.-H. (1992) The Pas2 protein essential for peroxisome biogenesis is related to ubiquitin-conjugating enzymes. *Nature* **359**, 73–76
39. Crane, D. I., Kalish, J. E., and Gould, S. J. (1994) The *Pichia pastoris PAS4* gene encodes a ubiquitin-conjugating enzyme required for peroxisome assembly. *J. Biol. Chem.* **269**, 21835–21844
40. Klei, I. J.v. d., Hilbrands, R. E., Kiel, J. A. K. W., Rasmussen, S. W., Cregg, J. M., and Veenhuis, M. (1998) The ubiquitin-conjugating enzyme Pex4p of *Hansenula polymorpha* is required for efficient functioning of the PTS1 import pathway. *EMBO J.* **17**, 3608–3618
41. Scheffner, M., Nuber, U., and Huibregtse, J. M. (1995) Protein ubiquitination involving an E1-E2-E3 enzyme ubiquitin thioester cascade. *Nature* **373**, 81–83
42. Wu, P. Y., Hanlon, M., Eddins, M., Tsui, C., Rogers, R. S., Jensen, J. P., *et al.* (2003) A conserved catalytic residue in the ubiquitin-conjugating enzyme family. *EMBO J.* **22**, 5241–5250
43. Platta, H. W., Girzalsky, W., and Erdmann, R. (2004) Ubiquitination of the peroxisomal import receptor Pex5p. *Biochem. J.* **384**, 37–45
44. Kragt, A., Voorn-Brouwer, T., Berg, M.v. d., and Distel, B. (2005) The *Saccharomyces cerevisiae* peroxisomal import receptor Pex5p is monoubiquitinated in wild type cells. *J. Biol. Chem.* **280**, 7867–7874
45. Kiel, J. A. K. W., Emmrich, K., Meyer, H. E., and Kunau, W.-H. (2005) Ubiquitination of the peroxisomal targeting signal type 1 receptor, Pex5p, suggests the presence of a quality control mechanism during peroxisomal matrix protein import. *J. Biol. Chem.* **280**, 1921–1930
46. Goto-Yamada, S., Mano, S., Nakamori, C., Kondo, M., Yamawaki, R., Kato, A., *et al.* (2014) Chaperone and protease functions of LON protease 2 modulate the peroxisomal transition and degradation with autophagy. *Plant Cell Physiol.* **55**, 482–496
47. Kato, A., Hayashi, M., Takeuchi, Y., and Nishimura, M. (1996) cDNA cloning and expression of a gene for 3-ketoacyl-CoA thiolase in pumpkin cotyledons. *Plant Mol. Biol.* **31**, 843–852
48. Hayashi, M., Toriyama, K., Kondo, M., and Nishimura, M. (1998) 2,4-Dichlorophenoxybutyric acid-resistant mutants of Arabidopsis have defects in glyoxysomal fatty acid β-oxidation. *Plant Cell* **10**, 183–195
49. Winter, D., Vinegar, B., Nahal, H., Ammar, R., Wilson, G. V., and Provart, N. J. (2007) An "Electronic Fluorescent Pictograph" browser for exploring and analyzing large-scale biological data sets. *PLoS One* **2**, e718
50. Hershko, A., Heller, H., Elias, S., and Ciechanover, A. (1983) Components of ubiquitin-protein ligase system. Resolution, affinity purification, and role in protein breakdown. *J. Biol. Chem.* **258**, 8206–8214
51. Kaplan, C. P., Thomas, J. E., Charlton, W. L., and Baker, A. (2001) Identification and characterisation of PEX6 orthologues from plants. *Biochim. Biophys. Acta* **1539**, 173–180
52. Gonzalez, K. L., Ratzel, S. E., Burks, K. H., Danan, C. H., Wages, J. M., Zolma, B. K., *et al.* (2018) A pex1 missense mutation improves peroxisome function in a subset of Arabidopsis pex6 mutants without restoring PEX5 recycling. *Proc. Natl. Acad. Sci. U. S. A.* **115**, E3163–E3172
53. Sparkes, I. A., Brandizzi, F., Slocombe, S. P., El-Shami, M., Hawes, C., and Baker, A. (2003) An Arabidopsis *pex10* null mutant is embryo lethal, implicating peroxisomes in an essential role during plant embryogenesis. *Plant Physiol.* **133**, 1809–1819
54. Sparkes, I. A., Hawes, C., and Baker, A. (2005) *At*Pex2 and *At*Pex10 are targeted to peroxisomes independently of known endoplasmic reticulum trafficking routes. *Plant Physiol.* **139**, 690–700
55. Prestele, J., Hierl, G., Scherling, C., Hetkamp, S., Schwechheimer, C., Isono, E., *et al.* (2010) Different functions of the C_3HC_4 zinc RING finger peroxins PEX10, PEX2, and PEX12 in peroxisome formation and matrix protein import. *Proc. Natl. Acad. Sci. U. S. A.* **107**, 14915–14920
56. Burkhart, S. E., Kao, Y. T., and Bartel, B. (2014) Peroxisomal ubiquitin-protein ligases peroxin2 and peroxin10 have distinct but synergistic roles in matrix protein import and peroxin5 retrotranslocation in Arabidopsis. *Plant Physiol.* **166**, 1329–1344
57. Dodt, G., and Gould, S. J. (1996) Multiple PEX genes are required for proper subcellular distribution and stability of Pex5p, the PTS1 receptor: evidence that PTS1 protein import is mediated by a cycling receptor. *J. Cell Biol.* **135**, 1763–1774
58. Kerssen, D., Hambruch, E., Klaas, W., Platta, H. W., Kruijff, B.d., Erdmann, R., *et al.* (2006) Membrane association of the cycling peroxisome import receptor Pex5p. *J. Biol. Chem.* **281**, 27003–27015
59. Kao, Y. T., and Bartel, B. (2015) Elevated growth temperature decreases levels of the PEX5 peroxisome-targeting signal receptor and ameliorates defects of Arabidopsis mutants with an impaired PEX4 ubiquitin-conjugating enzyme. *BMC Plant Biol.* **15**, 224
60. Carvalho, A. F., Pinto, M. P., Grou, C. P., Alencastre, I. S., Fransen, M., Sá-Miranda, C., *et al.* (2007) Ubiquitination of mammalian Pex5p, the peroxisomal import receptor. *J. Biochem.* **282**, 31267–31272
61. Platta, H. W., Magraoui, F. E., Schlee, D., Grunau, S., Girzalsky, W., and Erdmann, R. (2007) Ubiquitination of the peroxisomal import receptor Pex5p is required for its recycling. *J. Cell Biol.* **177**, 197–204
62. Philip, N., and Haystead, T. A. (2007) Characterization of a UBC13 kinase in *Plasmodium falciparum*. *Proc. Natl. Acad. Sci. U. S. A.* **104**, 7845–7850
63. Sato, T., Maekawa, S., Yasuda, S., Domeki, Y., Sueyoshi, K., Fujiwara, M., *et al.* (2011) Identification of 14-3-3 proteins as a target of ATL31 ubiquitin ligase, a regulator of the C/N response in Arabidopsis. *Plant J.* **68**, 137–146
64. Mural, R. V., Liu, Y., Rosebrock, T. R., Brady, J. J., Hamera, S., Connor, R. A., *et al.* (2013) The tomato Fni3 lysine-63-specific ubiquitin-conjugating enzyme and suv ubiquitin E2 variant positively regulate plant immunity. *Plant Cell* **25**, 3615–3631

65. Zhou, B., Mural, R. V., Chen, X., Oates, M. E., Connor, R. A., Martin, G. B., *et al.* (2017) A subset of ubiquitin-conjugating enzymes is essential for plant immunity. *Plant Physiol.* **173**, 1371–1390
66. Kraft, E., Stone, S. L., Ma, L., Su, N., Gao, Y., Lau, O.-S., *et al.* (2005) Genome analysis and functional characterization of the E2 and RING-type E3 ligase ubiquitination enzymes of Arabidopsis. *Plant Physiol.* **139**, 1597–1611
67. Mano, S., Nakamori, C., Hayashi, M., Kato, A., Kondo, M., and Nishimura, M. (2002) Distribution and characterization of peroxisomes in Arabidopsis by visualization with GFP: dynamic morphology and actin-dependent movement. *Plant Cell Physiol.* **43**, 331–341
68. Nakagawa, T., Suzuki, T., Murata, S., Nakamura, S., Hino, T., Maeo, K., *et al.* (2007) Improved gateway binary vectors: high-performance vectors for creation of fusion constructs in transgenic analysis of plants. *Biosci. Biotechnol. Biochem.* **71**, 2095–2100
69. Nakagawa, T., Nakamura, S., Tanaka, K., Kawamukai, M., Suzuki, T., Nakamura, K., *et al.* (2008) Development of R4 Gateway binary bectors (R4pGWB) enabling high-throughput promoter swapping for plant research. *Biosci. Biotechnol. Biochem.* **72**, 624–629
70. Bechtold, N., Ellis, J., and Pelletier, G. (1993) *In Planta Agrobacterium* mediated gene transfer by infiltration of adult *Arabidopsis thaliana* plants. *C. R. Acad. Sci. Paris, Life Sci.* **316**, 1194–1199
71. Tanaka, Y., Shibahara, K., and Nakagawa, T. (2013) Development of Gateway binary bectors R4L1pGWB possessing the bialaphos resistance gene (bar) and the tunicamycin resistance gene as markers for promoter analysis in plants. *Biosci. Biotechnol. Biochem.* **77**, 1795–1797
72. Hayashi, M., Toriyama, K., Kondo, M., Hara-Nishimura, I., and Nishimura, M. (1999) Accumulation of a fusion protein containing 2S albumin induces novel vesicles in vegetative cells of *Arabidopsis*. *Plant Cell Physiol.* **40**, 263–272
73. Asano, T., Yoshioka, Y., Kurei, S., Sakamoto, W., Sodmergen, and Machida, Y. (2004) A mutation of the *CRUMPLED LEAF* gene that encodes a protein localized in the outer envelope membrane of plastids affects the pattern of cell division, cell differentiation, and plastid in *Arabidopsis*. *Plant J.* **38**, 448–459
74. Koumoto, Y., Shimada, T., Kondo, M., Takao, T., Shimonishi, Y., Hara-Nishimura, I., *et al.* (1999) Chloroplast Cpn20 forms a tetrameric structure in *Arabidopsis thaliana*. *Plant J.* **17**, 467–477
75. Hayashi, Y., Hayashi, M., Hayashi, H., Hara-Nishimura, I., and Nishimua, M. (2001) Direct interaction between glyoxysomes and lipid bodies in cotyledons of the *Arabidopsis thaliana ped1* mutant. *Protoplasma* **218**, 83–94